EJN fens European Journal of Neuroscience

European Journal of Neuroscience, Vol. 33, pp. 868–878, 2011 doi:10.1111/j.1460-9568.2010.07552.x

SYNAPTIC MECHANISMS

Differential localization of $GABA_A$ receptor subunits in relation to rat striatopallidal and pallidopallidal synapses

A. Gross,[1,2] R. E. Sims,[1] J. D. Swinny,[3] W. Sieghart,[4] J. P. Bolam[2] and I. M. Stanford[1]
[1]Aston University, School of Life and Health Sciences, Birmingham, UK
[2]MRC Anatomical Neuropharmacology Unit, Dept of Pharmacology, Oxford, UK
[3]University of Portsmouth, School of Pharmacy and Biomedical Sciences, Portsmouth, UK
[4]Medical University of Vienna, Vienna, Austria

Keywords: globus pallidus, immunofluorescence, zolpidem

Abstract

As a central integrator of basal ganglia function, the external segment of the globus pallidus (GP) plays a critical role in the control of voluntary movement. The GP is composed of a network of inhibitory GABA-containing projection neurons which receive GABAergic input from axons of the striatum (Str) and local collaterals of GP neurons. Here, using electrophysiological techniques and immunofluorescent labeling we have investigated the differential cellular distribution of α1, α2 and α3 $GABA_A$ receptor subunits in relation to striatopallidal (Str-GP) and pallidopallidal (GP-GP) synapses. Electrophysiological investigations showed that zolpidem (100 nM; selective for the α1 subunit) increased the amplitude and the decay time of both Str-GP and GP-GP IPSCs, indicating the presence of the α1 subunits at both synapses. However, the application of drugs selective for the α2, α3 and α5 subunits (zolpidem at 400 nM, L-838,417 and TP003) revealed differential effects on amplitude and decay time of IPSCs, suggesting the nonuniform distribution of non-α1 subunits. Immunofluorescence revealed widespread distribution of the α1 subunit at both soma and dendrites, while double- and triple-immunofluorescent labeling for parvalbumin, enkephalin, gephyrin and the γ2 subunit indicated strong immunoreactivity for $GABA_A$ α3 subunits in perisomatic synapses, a region mainly targeted by local axon collaterals. In contrast, immunoreactivity for synaptic $GABA_A$ α2 subunits was observed in dendritic compartments where striatal synapses are preferentially located. Due to the kinetic properties which each $GABA_A$ α subunit confers, this distribution is likely to contribute differentially to both physiological and pathological patterns of activity.

Introduction

The basal ganglia (BG) consist of a group of nuclei involved in a variety of functions, including motor control, and are the principal site of pathology in a variety of diseases including Parkinson's disease. Driven by intrinsic mechanisms and excitatory glutamatergic inputs from the subthalamic nucleus (STN), neurons of the globus pallidus (GP; external segment of the globus pallidus in primates) process and transmit information from the striatum to the STN (Smith *et al.*, 1990; Parent & Hazrati, 1995), the internal segment of the globus pallidus (Kincaid *et al.*, 1991), the substantia nigra pars reticulata (Smith & Bolam, 1989) and the striatum (Bevan *et al.*, 1998). Neurons of the GP are thus in a position to powerfully influence activity of the whole BG (Bolam *et al.*, 2000).

The GP is composed of a network of inhibitory GABAergic projection neurons. Ninety per cent of their afferent synapses are GABAergic, arising from the striatum and the axon collaterals of neighbouring GP neurons. The GP boutons preferentially innervate the soma and proximal dendrites of GP neurons (Kita & Kitai, 1994; Sato *et al.*, 2000) in the form of perineuronal nets (Shink *et al.*, 1996; Sadek *et al.*, 2007). Electrophysiological studies (Sims *et al.*, 2008) have revealed significant differences in the characteristics of striatopallidal (Str-GP) and pallidopallidal (GP-GP) synapses which may be due to differential expression of $GABA_A$ subunits.

$GABA_A$ receptors are heteropentameric channels composed of a family of receptor subunits. Functional $GABA_A$ receptors require the co-assembly of 2α, 2β and one other subunit (Barnard, 1995; Tretter *et al.*, 1997; Farrar *et al.*, 1999), the most common form being composed of 2α, 2β and 1γ (Ernst *et al.*, 2003; Benke *et al.*, 2004). Different subunits confer different pharmacological and electrophysiological properties (Sieghart, 1995). Thus, receptors containing the α1 subunit have fast deactivation and desensitization kinetics (Freund & Buzsaki, 1996; Klausberger *et al.*, 2002) whereas those containing the α2 subunit show rapid activation but slow deactivation rates (Lavoie *et al.*, 1997) and an apparent 10-fold higher affinity for GABA (Levitan *et al.*, 1988). The β subunit appears to be an integral part of the recognition site for GABA (Amin & Weiss, 1993) and has a role in receptor desensitization (Newell & Dunn, 2002) while the γ subunit, together with the α subunit, is associated with the benzodiazepine-binding site (Sieghart, 1995; Sigel, 2002; Ernst *et al.*, 2003) and is implicated in clustering at synaptic sites through interaction

Correspondence: Ian M. Stanford, as above.
E-mail: I.M.Stanford@aston.ac.uk

Received 1 October 2010, revised 4 November 2010, accepted 8 November 2010

with the microtubule protein gephyrin (Ramming *et al.*, 2000; Fritschy *et al.*, 2008).

Previous reports indicate dense immunoreactivity for $GABA_A$ $\alpha1$, $\beta2$ and $\gamma1$ subunits and weaker immunoreactivity for $GABA_A$ $\alpha2$, $\alpha3$, $\beta3$ and $\gamma2$ subunits (Fritschy *et al.*, 1992; Fritschy & Mohler, 1995; Pirker *et al.*, 2000; Schwarzer *et al.*, 2001) in the GP. In this study, our aim was to determine whether different $GABA_A$ receptor subunits are selectively associated with Str-GP and GP-GP synapses and thus underlie differences in the properties of the synapses. This was done by a combination of electrophysiological, pharmacological and immunofluorescence analyses.

Materials and methods

All the animals in this study were used in accordance with the Animals (Scientific Procedures) Act, 1986 (UK) and in accordance with the European Community Council Directive of 24th November 1986 (86/609/EEC).

Electrophysiology

The 18- to 22-day-old male Wistar rats used in this study were inbred from a colony originally obtained from Charles River (Kent, UK). Rats were first anaesthetized with isoflurane in 2% O_2 until cardiorespiratory arrest and then decapitated. Brain slices (300 μm) were then cut on a DTK-1000 Microslicer (Dosaka, Japan) in a sucrose-based solution comprising (in mM): sucrose, 206; KCl, 2.5; $CaCl_2.2H_2O$, 1; $NaHCO_3$, 26; NaH_2PO_4, 1.25; $MgCl_2.6H_2O$, 2; glucose, 10; and indomethacin, 0.045. The slices were then incubated at room temperature for 1 h in artificial cerebrospinal fluid (aCSF) comprising (in mM): NaCl, 126; KCl, 2.5; $CaCl_2.2H_2O$, 2; $NaHCO_3$, 26; NaH_2PO_4, 1.2; $MgCl_2.6H_2O$, 1.3; and glucose, 10. The cutting solution and aCSF were equilibrated with 95 : 5% O_2 : CO_2 and had pH 7.4. Slices were then transferred to a recording chamber perfused with aCSF at a rate of 2 mL/min, at 32 °C. Neurons were visualized by differential interference contrast infrared microscopy with an Olympus BX51W1 microscope together with a CCD KP-M1 camera (Hitachi, Japan).

Whole-cell patch-clamp recordings were made using borosilicate glass pipettes (1.5–2.5 MΩ resistance) and filled with a chloride-based internal solution, comprising (in mM): KCl, 125; NaCl; 10, $CaCl_2$, 1; $MgCl_2$, 2; HEPES, 10; GTP, 0.3; Mg-ATP, 2; and BAPTA, 10 (adjusted to pH 7.3 with KOH).

Membrane currents were recorded in neurons voltage-clamped at −80 mV using an Axopatch 700 A patch-clamp amplifier (Molecular Devices, USA). Series resistance (3–20 MΩ) was monitored throughout experiments and compensated by > 60%. Results from neurons whose series resistance changed by > 20% throughout the analysis, or was > 20 MΩ, were discarded.

Focal stimulation was applied with glass electrodes filled with aCSF, and carried out using a DS-3 isolated stimulator (Digitimer, UK) with pulses of 0.1 ms width and 0.02–1 mA at 0.2 Hz. To block NMDA and AMPA receptors that may have been activated by glutamatergic inputs from the STN or possibly the pedunculopontine nucleus, 50 μM 2-AP5 and 10 μM CNQX was routinely added to the aCSF. Selective stimulation of Str-GP synapses and GP-GP synapses was achieved as described previously (Sims *et al.*, 2008). In brief, for the stimulation of Str-GP connections, sagittal sections were used and electrodes were placed in dense axonal bundles within the striatum itself. For the stimulation of GP-GP connections coronal sections were used, thus reducing the impact of Str-GP inputs. In these experiments stimulating electrodes were placed in the GP itself, away from striatopallidal axonal bundles but within 200 μm of the recorded GP neuron.

The use of sagittal and coronal sections to separate Str-GP inputs from GP-GP inputs is based upon the knowledge that Str-GP projections project along the rostrocaudal axis (Wilson & Phelan, 1982) and that the dendritic arbor of many GP neurons lies perpendicular to this striatal input (Kita & Kitai, 1994). These planes of section have been used previously to separate Str-GP inputs from GP-GP inputs and show differential sensitivity to dopamine D2 agonists (Cooper & Stanford, 2000) and Str-GP sensitivity to cannabinoid CB1 agonists (Engler *et al.*, 2006).

Striatal inputs are therefore effectively negated in slices cut in the coronal plane, allowing stimulation of GP-GP inputs without extensive contamination. However, cross-stimulation is still a possibility as up to 30% of GP neurons project back to the striatum (Bevan *et al.*, 1998). Thus, there was the potential that striatal stimulation could antidromically activate GP axons which would contaminate presumed Str-GP responses. Antidromic responses were occasionally observed but were easily identified as the amplitude was directly proportional to stimulation intensity and peaked within 0.1 ms of the stimulation artefact. All data showing evidence of antidromic activity were discarded. We acknowledge that antidromic stimulation of other GP cells may take place, which may then release GABA onto our recorded cell. However, the precise location and stimulation strength was manipulated to evoke inhibitory postsynaptic currents (IPSCs) without failures and without multiple peaks which may arise through stimulation of multiple fibres and/or the activation of polysynaptic networks.

Data were recorded at 10 kHz, filtered with an eight-pole low-pass Bessel filter at 4 kHz using a Multiclamp 700 A amplifier, and digitized with a Digidata 1322 A. Analysis was performed online with CLAMPEX 9.2 and offline using CLAMPFIT 9.2 (all Molecular Devices). The amplitude of each IPSC was measured from a point immediately before the stimulation artefact while decay times were calculated by fitting single exponential curves in CLAMPFIT 9.2. In the data traces presented, stimulation artefacts were removed offline. All data is expressed as mean ± SEM unless otherwise stated. The Mann–Whitney *U*-test was used to assess differences from baseline recordings 15 min after drug application, and $P < 0.05$ was considered significant.

Drugs

2-AP5 and CNQX were supplied by Ascent Scientific (UK), diazepam (non-selective benzodiazepine) from Sigma UK and zolpidem (selective for the $GABA_A$ $\alpha1$ subunit) and L-838,417 (selective efficacy for $GABA_A$ $\alpha2$, $\alpha3$ and $\alpha5$ subunits) from Tocris (UK). TP003 ($GABA_A$ $\alpha3$ subunit selective agonist) was supplied by and used with the permission of Merck Research Laboratories (NJ, USA). All drugs were initially made in 1000 × stock solutions and diluted to the final concentration in aCSF immediately prior to application.

Immunofluorescent labeling

Immunofluorescent localization of $GABA_A$ receptor subunits can often yield false-negative or nonspecific labeling as some of these proteins are sensitive to the aldehyde concentrations used in the fixation process. Therefore, we optimised our fixation protocol to reach the most ideal labeling, using 1% paraformaldehyde and low pH fixation for the $\alpha3$ experiments, and 2% paraformaldehyde in combination with pepsin digestion for all the other immunoreactions.

Six adult Sprague–Dawley rats (250–450 g; Charles River, Margate, UK) were used. Each animal was anesthetized with phenobarbital, and perfused with ~50 mL of phosphate-buffered saline (PBS; 0.01 M phosphate buffer, pH 7.4, 0.876% NaCl, 0.02% KCl) via the ascending aorta, followed by ~200 mL of fixative (0.1 M phosphate buffer, pH 7.4, 1 or 2% paraformaldehyde, 15% saturated picric acid) over a period of 25 min. For the $GABA_A$ α3 subunit experiments the fixative consisted of 1% paraformaldehyde in Na-acetate buffer at pH 6. Free fixative was removed by post-perfusion with PBS. The brains were removed and 60-μm sagittal sections cut using a vibrating blade microtome (VT1000S; Leica).

Sections for most of the immunoreactions (except the reactions with the α3 antibody, where no pepsin treatment was used) were washed in 0.1 M phosphate buffer, and then treated with 0.02% pepsin (P-7125; Sigma-Aldrich Chemie, Steinheim, Germany) to unmask the antigens and epitopes, thus enhancing staining intensity. Sections were preincubated for 2 h at room temperature in blocking solution, consisting of 20% normal donkey serum, 0.2% Triton X-100 in Tris-buffered saline (TBS; 50 mM, pH 7.5, 0.9% NaCl). This was followed by overnight incubation at 4 °C with one or more primary antibodies against: $GABA_A$ subunits (α1, α2, α3, γ2), gephyrin, parvalbumin, enkephalin, vesicular GABA transporter (VGAT) and anti-human neuronal protein (anti-HuC/D). Details of the origin, specificity and dilutions of antibodies are given in Table 1.

Sections were then washed and incubated in mixture of fluorescent-tagged secondary antibodies. Finally, sections were washed, mounted and cover-slipped using fluorescence mounting medium (Vectashield; Vector Laboratories, Inc., Burlingame, CA, USA).

Controls

The specificity of $GABA_A$ α1, α2, α3 and γ2 antibodies have all been previously tested in knockout animals (see Table 1 for references). To test for cross-reactivity between various antibodies, sections were processed with a full complement of secondary antibodies and one primary antibody at a time. None of the combinations with species-unrelated secondary antibodies resulted in labeling. In addition, no selective labeling was found in sections incubated with combinations of secondary antibodies without a primary antibody (see Supporting Information Table S1).

Imaging and data acquisition

Images were captured with an LSM 710 (Zeiss, Göttingen Germany) confocal microscope with Plan-Apochromat 63 × /1.40 oil and 40 × /1.3 or 20 × objectives. For low magnification LSM images a 10 × objective was used. The ZEN 2008 software's default settings for the fluorophors were used for beam splitters and ranges of emissions sampled. Two-channel *z*-stacks were acquired using the System Random Sampling (SRS) automatic acquisition function, following a manual prefocussing step at all capture sites, and projection images were analyzed. However, for better quality, single images are presented in the figures. For stereological analysis, three sections from two animals were analyzed using a fluorescence-capable Stereo-Investigator system (MBF Biosciences, MicroBrightField Europe, Magdeburg, Germany). The boundary of the GP was drawn at low (10 × objective) magnification. A sampling grid was randomly positioned over the GP contour. The sizes of grids were chosen according to the abundance of analyzed neurons (240 × 180 μm for α1-HuC/D and 375 × 270 μm for α1-gephyrin experiments). A counting frame of 125 × 90 μm was located at the top left of each grid cell.

Results

IPSCs were evoked either by stimulation within the GP in coronal slices selectively activating GP-GP synapses or by stimulation in the striatum in sagittal slices selectively activating Str-GP synapses. Previous studies (Sims *et al.*, 2008) have revealed differences in the kinetics of these evoked IPSCs and this was confirmed in the current experiments. Thus, rise times, decay times and half-widths of Str-GP responses were significantly slower than those of GP-GP synapses, data which is consistent with local collaterals innervating the soma and proximal dendrites of GP neurons and striatal inputs preferentially innervating more distal regions.

In the first series of experiments the non-subunit-selective benzodiazepine, diazepam, was used. Diazepam (500 nM) increased the Str-GP evoked IPSC amplitude (130.7 ± 10.3%, $n = 6$, $P = 0.0006$; Mann–Whitney *U*-test) and GP-GP evoked IPSC amplitude (141.3 ± 15.4%, $n = 6$, $P = 0.0012$; Mann–Whitney *U*-test) after 15 min application (Fig. 1, A/1 and A/2). As expected from a benzodiazepine-mediated action, the decay time of the Str-GP and

TABLE 1. Details of primary and secondary antibodies

Primary antibodies				Secondary antibodies			No of	
Against	Species	Dilution	Source and characterization	Antibody	Dilution	Source	Sections	Animals
$GABA_A$α1	Rabbit	1 : 10000	Fritschy & Mohler (1995)	Donkey-α-rb Alexa 488 Donkey-α-rb CY5	1 : 1000 1 : 250	Invitrogen, Molecular Probes Jackson Laboratories	10	5
$GABA_A$α2	Rabbit	1 : 1000	Kasugai *et al.*, (2010)	Donkey-α-rb Alexa 488	1 : 1000	Invitrogen, Molecular Probes	5	3
$GABA_A$α3	Guinea-pig	1 : 4000	Fritschy & Mohler (1995)	Donkey-α-gp CY3	1 : 400	Jackson Laboratories	8	4
$GABA_A$ γ2	Rabbit	1 : 200	Kasugai *et al.*, (2010)	Donkey-α-rb Alexa 488	1 : 1000	Invitrogen, Molecular Probes	3	3
$GABA_A$ γ2	Guinea-pig	1 : 250	Fritschy & Mohler (1995)	Donkey-α-gp CY3	1 : 400	Jackson Laboratories	3	3
Gephyrin	Mouse	1 : 1000	Synaptic Systems #mAB7a Schneider Gasser *et al.* (2006) Jacob *et al.* (2005)	Donkey-α-m CY3	1 : 400	Jackson Laboratories	10	5
Parvalbumin	Guinea-pig	1 : 1000	Synaptic Systems #195 004	Donkey-α-gp CY5	1 : 250	Jackson Laboratories	5	3
Enkephalin	Mouse	1 : 500	Chemicon #MAB 350 Lindemeyer *et al.*, (2006)	Donkey-α-m CY3	1 : 400	Jackson Laboratories	5	3
HuC/D	Mouse	1 : 100	Molecular Probes #A-21271 Fornaro & Geuna (2005)	Donkey-α-m CY5	1 : 250	Jackson Laboratories	3	3
VGAT	Guinea-pig	1 : 500	Synaptic Systems #131 005 Gronborg *et al.* (2010)	CY5	1 : 250	Jackson Laboratories	4	2

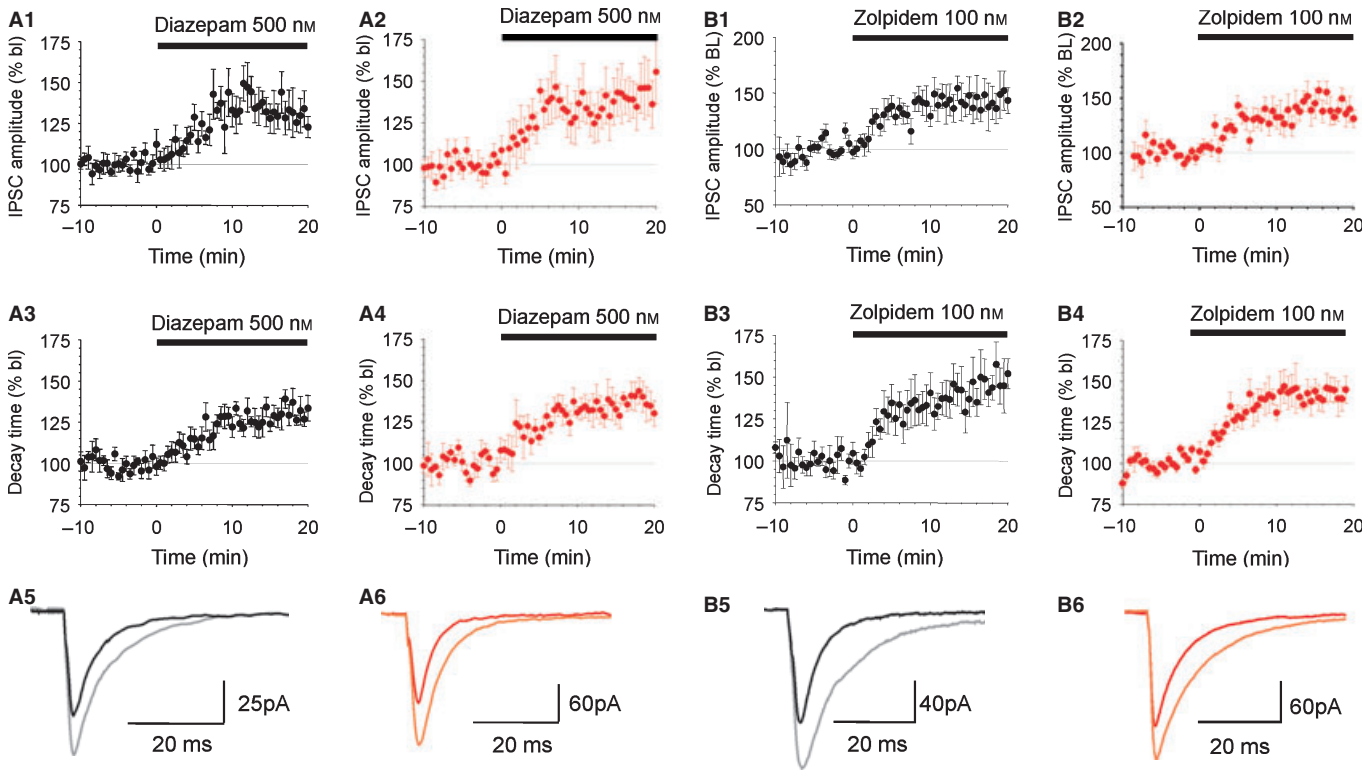

FIG. 1. The α1 subunit was widely distributed in GP and was present at both Str-GP and GP-GP synapses. (A) Diazepam (500 nM) was added after 10 min baseline recording. At both Str-GP (n = 6, black) and GP-GP (n = 6, red) synapses the IPSC amplitude (A/1 and A/2) and decay times (A/3 and A/4) were significantly increased. Each point represents the average of six responses. Data traces (once again, average of six) are shown for baseline (dark) and after 15 min diazepam (light) for both Str-GP (A/5) and GP-GP (A/6) synapses. (B) 100 nM zolpidem (selective for α1 GABA$_A$ subunits) was added 10 min after baseline recording. At both Str-GP (n = 6, black) and GP-GP (n = 6, red) synapses the IPSC amplitude (B/1 and B/2) and decay times (B/3 and B/4) were significantly increased. Data traces (average of six) are shown for baseline (dark) and after 15 min zolpidem (light) for both Str-GP (B/5) and GP-GP (B/6) synapses.

GP-GP evoked responses also significantly increased (129.0 ± 5.5%, n = 6, P = 0.0006 and 132.4 ± 8.9%, n = 6, P = 0.0012, respectively; Mann–Whitney U-test; Fig. 1, A/3 and A/4).

In order to probe for the presence of GABA$_A$ α1-subunit density at Str-GP and GP-GP synapses, zolpidem was used at 100 nM, a concentration at which it shows selectivity for the α1 subunit. At this concentration, zolpidem increased the Str-GP evoked IPSC amplitude (141.1 ± 13.7%, n = 6, P = 0.0012; Mann–Whitney U-test) and the GP-GP evoked IPSC amplitude (147.0 ± 12.3%, n = 6, P = 0.0012; Mann–Whitney U-test) after 15 min application (Fig. 1, B/1 and B/2). The decay time of the Str-GP and GP-GP evoked responses also increased compared to baseline (137.7 ± 12.5%, n = 6, P = 0.0221 and 140.7 ± 8.0%, n = 6, P = 0.0012, respectively; Mann–Whitney U-test; Fig. 1, B/3 and B/4). These data suggest that GABA$_A$ receptors containing the α1 subunit are located at both Str-GP and GP-GP synapses.

To complement the pharmacological data, we analyzed the cellular distribution of the GABA$_A$ α1 subunit. Strong immunoreactivity for the GABA$_A$ α1 subunit was detected throughout the GP (Fig. 2A). In order to determine the proportion of GP neurons that express the GABA$_A$ α1-subunit, double-labeling for the α1-subunit with the neuronal marker HuC/D was carried out and the numbers of single- and double-labeled neurons counted in a sample of three sections from two animals. From these counts, we estimate that 80.6% (710 of a total number 881 neurons counted) of the total population of GP neurons express GABA$_A$ α1 subunits and the expression of the subunit was not detected in 19.4%.

GP neurons can be characterized based on the expression of the calcium-binding protein parvalbumin. Therefore, to determine whether the receptor subunits are expressed in parvalbumin-negative or parvalbumin-positive GP neurons, we performed triple-labeling experiments for GABA$_A$ α1, gephyrin and parvalbumin (Fig. 2B–E). We found that the GABA$_A$ α1 subunit was co-localized with gephyrin and equally distributed on the soma (Fig. 2E, double arrowheads) and on dendrites of parvalbumin-positive and -negative GP neurons (Fig. 2E, arrowheads).

We acknowledge that the co-localization of gephyrin with the α1 subunit does not necessarily provide direct evidence for the synaptic location of the receptor subunit, as previous studies have reported both gephyrin-dependent and gephyrin-independent clustering of synaptic GABA$_A$ α1 subunit-containing receptors (Kneussel *et al.*, 2001; Lévi *et al.*, 2004). Indeed, this correlates with the observation that the population of GABA$_A$ α1-positive neurons expressed variable levels of gephyrin immunoreactivity within the soma. One group displayed only slightly stronger immunolabeling over background (Fig. 2C, asterisk), whereas the immunolabeling of the other group was considerably higher than background (Fig. 2E, arrows). This finding raises the question of whether neurons expressing low levels of gephyrin receive less inhibitory input, or express some other postsynaptic clustering protein. To address this question, triple-labeling immunofluorescent experiments were preformed with GABA$_A$α1, gephyrin and VGAT. Qualitative analysis revealed that in both the weak and strong gephyrin-immunoreactive neurons, immunoreactivities for the GABA$_A$ α1 (Supporting Information Fig. S1A) subunit and for VGAT (Supporting Information Fig. S1C) were equally strong (Supporting Information Fig. S1D). Thus, both weakly and strongly gephyrin-immunoreactive GP neurons may equally be targeted by putative GABAergic terminals, suggesting that

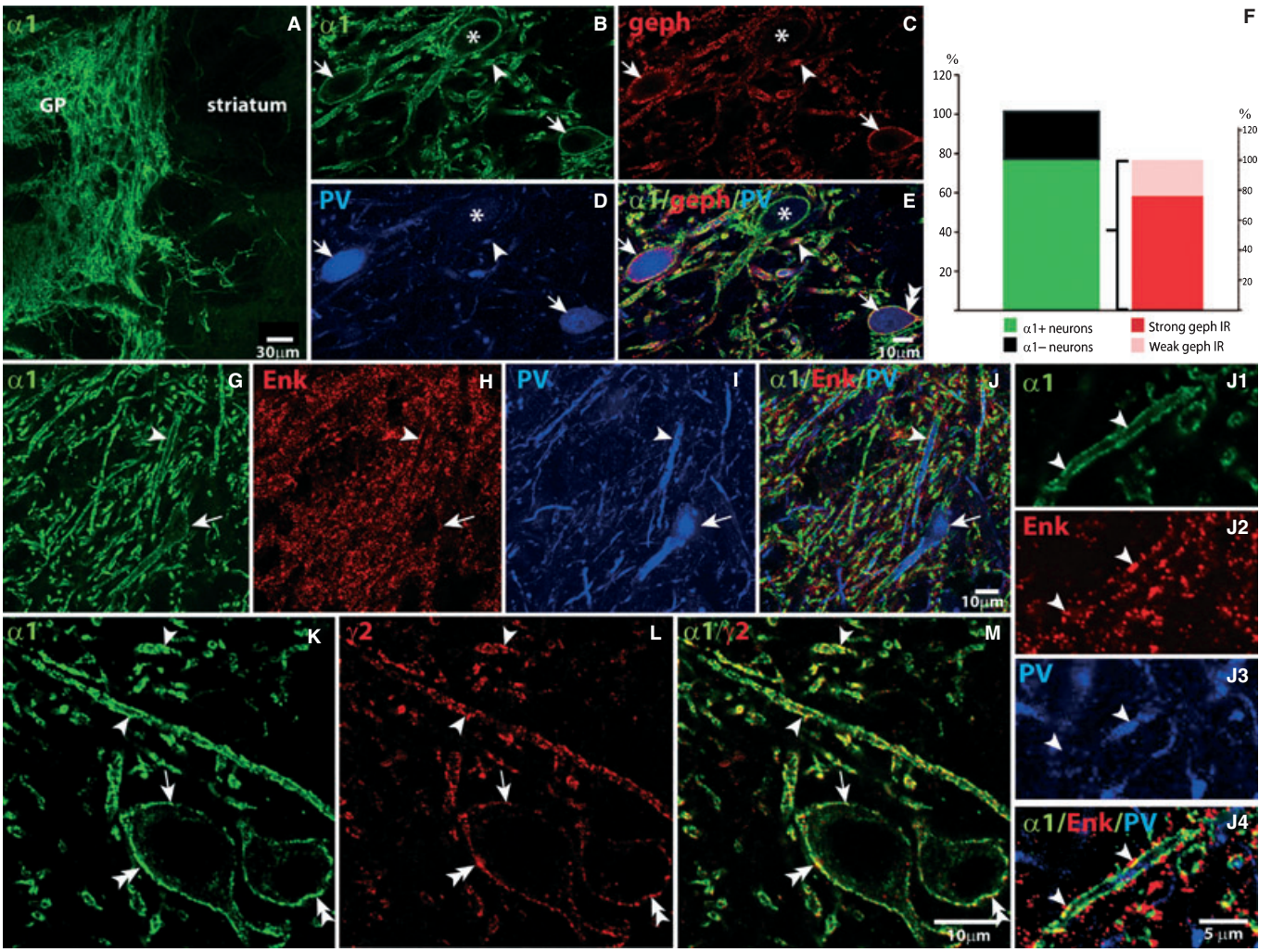

FIG. 2. $GABA_A$ α1 subunit immunoreactivity in globus pallidus neurons. (A) Low magnification confocal image showing strong immunoreactivity for the $GABA_A$ α1 subunit in GP and weak immunoreactivity in striatum. (B–E) Triple immunofluorescent labeling for the α1 subunit (green, B), gephyrin (red, C) and parvalbumin (blue, D). (B) $GABA_A$ α1 subunit immunoreactivity was widely distributed in the somata (arrows) and dendrites (arrowhead) of GP neurons. (C) GP neurons exhibited either strong (arrows) or weak (asterisk) gephyrin immunoreactivity. (D) Confocal image illustrating parvalbumin-positive (arrows) and -negative neurons (asterix) in GP. (E) Merged image showing that some $GABA_A$ α1 subunit-positive but parvalbumin-negative GP neurons (asterisk) showed strikingly weak immunoreactivity for gephyrin, whereas other neurons (arrows) and dendrites (arrowhead) were immunoreactive for all three markers. (F) Bar charts of the proportions of GP neurons expressing $GABA_A$ α1 subunit immunoreactivity (green) and the proportion of these that showed strong (red) and weak (pink) immunoreactivity for gephyrin. (G–J) Triple immunofluorescent labeling showing $GABA_A$ α1 subunit- and parvalbumin-positive neurons closely apposed by enkephalin-positive striatal axon terminals. (H) Confocal image illustrating very dense enkephalin immunoreactivity in GP associated with somata (arrow) and dendrites (arrowhead). (I) The same somata and dendrite as in H were immunopositive for parvalbumin. (J) Merged image showing $GABA_A$ α1 subunit and parvalbumin-positive cell bodies and dendrites closely apposed by many enkephalin-positive striatal axon terminals. (J/1–J/4) High magnification confocal images of the dendrite fragment indicated by an arrowhead in G–H showing the co-occurrence of $GABA_A$ α1 subunit immunoreactivity with presynaptic enkephalin immunoreactivity (arrowheads on J/4). (K–M): Confocal images of GP neurons expressing immunoreactivity for the $GABA_A$ α1 subunit co-localized with the $GABA_A$ γ2 subunit on somata (double arrowheads) and dendrites (arrowheads). Scale bar in E also applies to B–D; in G also applies to H–J; in J/4 also applies to J/1–J/3; in M also applies to K and L.

weakly gephyrin-positive GP neurons express some other protein besides gephyrin as a postsynaptic clustering protein.

Quantitative analysis of the $GABA_A$ α1-gephyrin double-labeling experiments revealed that 76% of α1-positive neurons in the GP are strongly positive for gephyrin (104 out of a total number of 136 neurons counted in three sections from two animals), as opposed to the remaining 24%, which are weakly positive for the synaptic marker (32 out of a total number 136 neurons counted in three sections from two animals; Fig. 2F). Interestingly, those neurons that showed strong immunoreactivity for gephyrin were also positive for parvalbumin (Fig. 2E, arrows), whereas neurons showing low levels of gephyrin immunoreactivity appeared to be parvalbumin-negative (Fig. 2E, asterisk).

In addition to double-labeling for gephyrin and $GABA_A$ α1, we performed further double-labeling experiments with antibodies against the $GABA_A$ γ2 subunit, which has also been shown to be required for postsynaptic clustering (Essrich *et al.*, 1998). These experiments revealed the co-location of the $GABA_A$ α1 subunits with the $GABA_A$ γ2 subunit at both somatic and dendritic locations (Fig. 2K–M), similar to what we found with gephyrin.

Additionally, we determined whether we could detect any preferential localization of the $GABA_A$ α1 subunit associated with striatal afferent terminals. In order to identify striatal terminals targeting GP neurons, we preformed double-labeling experiments with enkephalin antibodies. Taking into account that a small proportion of GP neurons have been shown to express preproenkephalin, a precursor of enkeph-

alin (Voorn *et al.*, 1999; Hoover & Marshall, 2002), it is still reasonable to suggest that the majority of the very dense enkephalin-immunoreactive terminals that are observed in GP are derived from the striatum (Fig. 2H). In all examined GABA$_A$ α1 subunit-expressing neurons, enkephalin immunoreactivity appeared to be distributed equally with somata and dendrites (Fig. 2, G–J and J/1–J/4). This suggests that the GABA$_A$ α1 subunit is equally associated with striatal and GP synapse, which is consistent with the electrophysiological data (see above).

At 100 nM, zolpidem is considered to be selective for GABA$_A$ receptors containing the α1 subunit whilst 400 nM zolpidem is considered non-selective, also having significant efficacy at GABA$_A$ α2 and α3 subunit-containing receptors (Langer *et al.*, 1992). In order to probe for the presence of GABA$_A$ receptors containing non-α1 subunits at Str-GP and GP-GP synapses, IPSC amplitude and decay time were monitored whilst raising the concentration of zolpidem from 100 to 400 nM (Fig. 3). This change in concentration had no effect on the amplitude of Str-GP IPSCs (94.4 ± 5.8%, $n = 8$, $P = 0.7308$; Mann–Whitney *U*-test; Fig. 3, A/1) but increased GP-GP IPSC amplitude (112.6 ± 3.7%, $n = 8$, $P = 0.0012$; Mann–Whitney *U*-test; Fig. 3, A/2) after 15 min application. However, the decay time of the evoked Str-GP and GP-GP IPSCs both increased, to 111.4 ± 3.0% ($n = 8$, $P = 0.0023$; Fig. 3, A/3) and 118.6 ± 5.4% ($n = 8$,

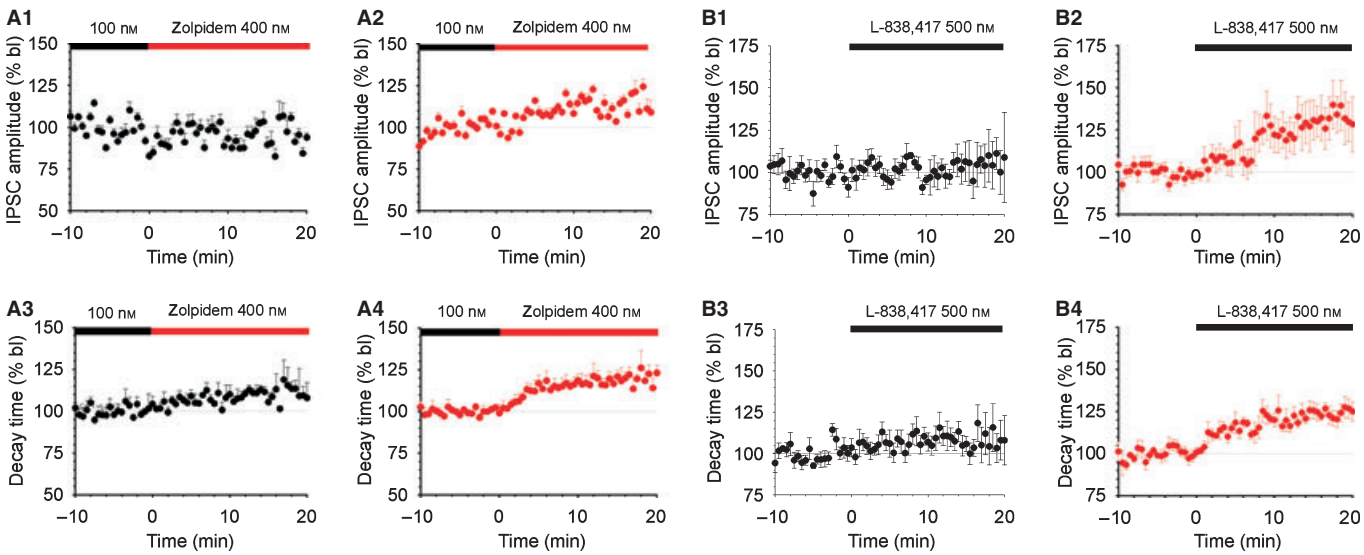

FIG. 3. A greater number of non-α subunits at GP-GP synapses. (A) 400 nM zolpidem was applied after 10 min baseline recording in 100 nM zolpidem. IPSC amplitude (A/1 and A/2) and decay times (A/3 and A/4) were significantly increased at GP-GP ($n = 8$, red) but not Str-GP ($n = 8$, black) synapses. (B) L-838,417 (500 nM) was added 10 min after baseline recording. Once again, IPSC amplitude (B/1 and B/2) and decay times (B/3 and B/4) were significantly increased at GP-GP ($n = 7$, red) but not Str-GP ($n = 6$, black) synapses.

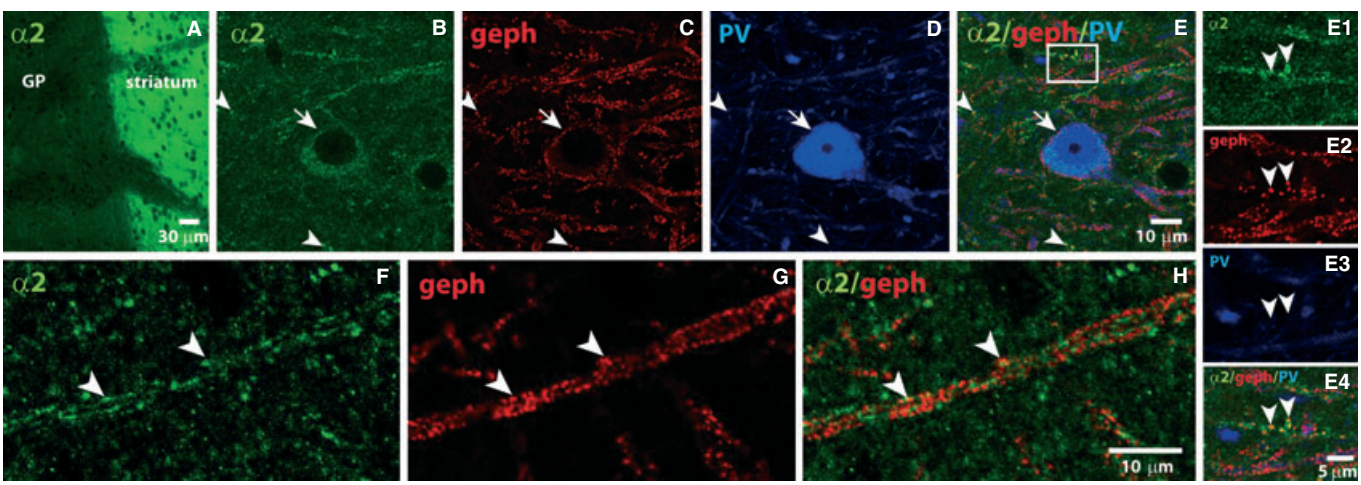

FIG. 4. GABA$_A$ α2 subunits were preferentially located in synapses targeting the dendrites of GP neurons. (A) Low power confocal image showing weak/moderate immunoreactivity for the GABA$_A$ α2 subunit in GP and strong labeling in striatum. (B–E) In GP, triple immunofluorescent images illustrating immunoreactivity for the GABA$_A$ α2 subunit (green) and gephyrin (red) in a parvalbumin-expressing (blue) GP neuron. (B) Confocal image showing strong, mainly intracellular, immunoreactivity for the α2 subunit in the soma (arrow), and punctate labeling in dendrites (arrowheads) of GP neurons. (C) Fluorescent image illustrating gephyrin immunoreactivity in somatic (arrow) and dendritic (arrowheads) compartments. (E) Merged image illustrating immunoreactivity for the GABA$_A$ α2 subunit (green) and gephyrin (red) in parvalbumin-expressing (blue) GP neuron somata (arrow) and dendrites (arrowheads). (E/1–E/4) High magnification images of the dendritic segment in the boxed area in E. Note the co-localization of the GABA$_A$ α2 subunit immunoreactivity (green) with gephyrin immunoreactivity (red; arrowheads in E/4). (F–H) High power confocal images illustrating the numerous GABA$_A$ α2 subunit puncta associated with the gephyrin labeling (F, green, arrowheads). Merged image in H. Scale bar in E also applies to B–D; in E/4 also applies to E/1–E/3; in H also applies to F and G.

$P = 0.0047$; Mann–Whitney *U*-test; Fig. 3, A/4) respectively. The greater effect on GP-GP IPSCs of raising zolpidem concentration to 400 nM suggests that there is a higher density of non-α1 subunits at GP-GP synapses. To further test these data, experiments were carried out with L-838,417, an anxiolytic non-benzodiazepine compound that has no efficacy at $GABA_A$ α1 subunits but acts as a partial agonist at α2, α3 and α5 subunits (McKernan *et al.*, 2000). L-838,417 (500 nM) had little effect on the amplitude of Str-GP IPSCs (104.5 ± 11.3%, $n = 6$, $P = 0.4452$; Mann–Whitney *U*-test; Fig. 3, B/1) or decay time (103.6 ± 5.7%, $n = 6$, $P = 0.6282$; Mann–Whitney *U*-test; Fig. 3, B/3), but significantly increased the amplitude (129.3 ± 12.1%, $n = 7$, $P = 0.0262$; Mann–Whitney *U*-test; Fig. 3, B/2) and decay time (125.2 ± 5.1%, $n = 7$, $P = 0.0005$; Mann–Whitney *U*-test Fig. 3, B/4) of GP-GP IPSCs.

To assess which non-α1 subunit is responsible for the enhancement of the amplitude and decay time at GP-GP synapses (Fig. 3), immunofluorescent labeling for the $GABA_A$ α2 subunit was carried out. Weak to moderate immunoreactivity for $GABA_A$ α2 was found throughout the GP (Fig. 4A). The majority of $GABA_A$ α2-positive neurons examined were once again positive for parvalbumin (Fig. 4D and E). Although immunoreactivity for the $GABA_A$ α2 subunit was found in both somatic and dendritic compartments of individual GP neurons (Fig. 4B and E/1), a clearly stronger immunoreactivity for the $GABA_A$ α2 subunit was observed in the dendrites (Fig. 4, E/1 and F).

Double-immunofluorescent labeling for the $GABA_A$ α2 subunit and gephyrin revealed well-defined co-localization in dendritic compartments with less pronounced co-localization at the soma. This suggests relatively more synaptic $GABA_A$ α2 subunits in the dendrites of GP neurons (Fig. 4E–H).

The observation that the $GABA_A$ α2 subunit appears preferentially located in dendritic compartments raises the question of which subunit is responsible for the increased GP-GP responses observed in the presence of 400 nM zolpidem and L-838,417? As zolpidem has been reported to be ineffective at $GABA_A$ α5 subunit-containing receptors (Pritchett & Seeburg, 1990; Langer *et al.*, 1992) the most likely candidate is the $GABA_A$ α3 subunit. In order to test this possibility, immunofluorescent labeling for the $GABA_A$ α3 subunit was carried out in combination with immunolabeling for α1 and γ2 subunits, enkephalin, parvalbumin and HuC/D (Fig. 5A–D). Weak to moderate immunoreactivity for $GABA_A$ α3 subunits was observed throughout the GP (Fig. 5A). The immunoreactivity for this subunit appeared to be both intracellular and membrane-associated. In contrast to the α2 subunit immunoreactivity, the α3 subunit appeared to be more pronounced at the soma than in dendritic compartments (Fig. 5B, E, H and L). Once again, gephyrin showed strong immunoreactivity throughout GP (Fig. 5F), whereas double labeling with $GABA_A$ α3 was mainly observed at the soma (Fig. 5G). Dense immunoreactivity for enkephalin was observed throughout the somatodendritic axis of GP neurons (Fig. 5I), immunoreactivity which was clearly associated with $GABA_A$ α3 subunit-positive and parvalbumin-positive neurons (Fig. 5K). Although immunoreactivity for the synaptic marker $GABA_A$ γ2 subunit was found at both somatic and dendritic locations, co-localization with the $GABA_A$ α3 subunit was mainly observed at the soma (Fig. 5L–N). As GP-GP synapses form perineuronal nets on the soma and proximal dendrites of GP cells (Shink *et al.*, 1996; Sadek *et al.*, 2007) it would be expected that the $GABA_A$ receptors containing the α3 subunit are preferentially targeted by local axon collaterals arising from other GP neurons.

To test for the presence of $GABA_A$ α3 subunits at GP-GP synapses we used the non-benzodiazepine TP003 (100 nM) which has significant selectivity at receptors containing α3 subunits (Dias *et al.*, 2005). After 15 min application of 100 nM TP003, IPSCs evoked in sagittal slices by stimulation of the striatum showed no significant change in amplitude (97.5 ± 4.8% $n = 7$, $P = 0.0973$; Mann–Whitney *U*-test; Fig. 6, A/1) or decay time (102.9 ± 5.8%, $n = 7$, $P = 0.0973$; Mann–Whitney *U*-test; Fig. 6, A/2). In contrast, IPSCs evoked in coronal slices by stimulation of GP showed significantly enhanced amplitude (125.0 ± 10.1%, $n = 7$, $P = 0.0023$; Mann–Whitney *U*-test; Fig. 6, B/1) without significant change in decay time (108.7 ± 5.9%, $n = 7$, $P = 0.0734$; Mann–Whitney *U*-test Fig. 6, B/2). These data provide further evidence of a role for the α3 subunit at GP-GP synapses.

Discussion

Neurons of the GP receive inhibitory GABAergic input from the striatum and also from neighbouring neurons. Although not as dense as the striatal input, GP-GP synapses mainly innervate the soma and proximal dendrites where they form synapses in a perisomatic basket-like pattern (Kita & Kitai, 1994; Sadek *et al.*, 2007). In this study we have used this feature to correlate the properties of somatic GP-GP synapses and widespread Str-GP synapses with specific $GABA_A$ α subunits.

Using zolpidem at a low concentration we have shown the $GABA_A$ α1 subunit to be present in both GP-GP and Str-GP synapses. Furthermore, immunocytochemical data reveal a widespread distribution of the $GABA_A$ α1 subunit, which is present in both dendritic and somatic compartments. It is likely that the majority of $GABA_A$ α1 subunits are located within the synapse as they co-localize with the synaptic markers gephyrin and the $GABA_A$ γ2 subunit. In contrast, the $GABA_A$ α2 and α3 subunits show a differential subcellular distribution. The α2 subunit appeared to be preferentially located at distal dendritic compartments, where it is co-localized with gephyrin, whereas immunoreactivity for the $GABA_A$ α3 subunit was confined to perisomatic regions where it co-localized with gephyrin and the γ2 subunit. Unfortunately, quantification of immunofluorescent puncta in GP was not possible due to the relatively poor labeling observed. This problem is most likely the anatomical properties of GP itself as simultaneous experiments using cortical and hippocampal tissue provided convincing punctate labeling with both the $GABA_A$ α2 and α3 antibodies. Quantification of these subunits was also attempted at the ultrastructural level using electron microscopic analysis; however, once again poor labeling limited our analysis. Therefore, we were restricted to a qualitative light microscopic analysis complemented by the pharmacological and electrophysiological data.

Cellular distribution

In brain slice preparations, medium spiny projection neurons of the striatum display hyperpolarized resting membrane potentials commonly around −90 mV and are therefore quiescent (Jiang & North, 1991). In contrast, the majority of GP neurons exhibit spontaneous activity (Nambu & Llinas, 1994; Cooper & Stanford, 2000). Based on the assumption that Str-GP inputs are more numerous, we initially thought that analysis of spontaneous action potential-driven IPSCs (arising from GP) and miniature IPSCs (the majority of which are presumed to be Str-GP in origin), should separate GP-GP and Str-GP activity. However, no kinetic differences between spontaneous and miniature IPSCS were observed, leaving little confidence in the use of this type of analysis in the separation of these inputs. However, significant differences in the kinetics of evoked IPSCs were observed in coronal and sagittal slices, indicating a better separation of GP-GP and Str-GP IPSCs. Thus, a typical GP-GP IPSC exhibits fast rise time, rapid decay and short half width while IPSCs elicited by Str-GP

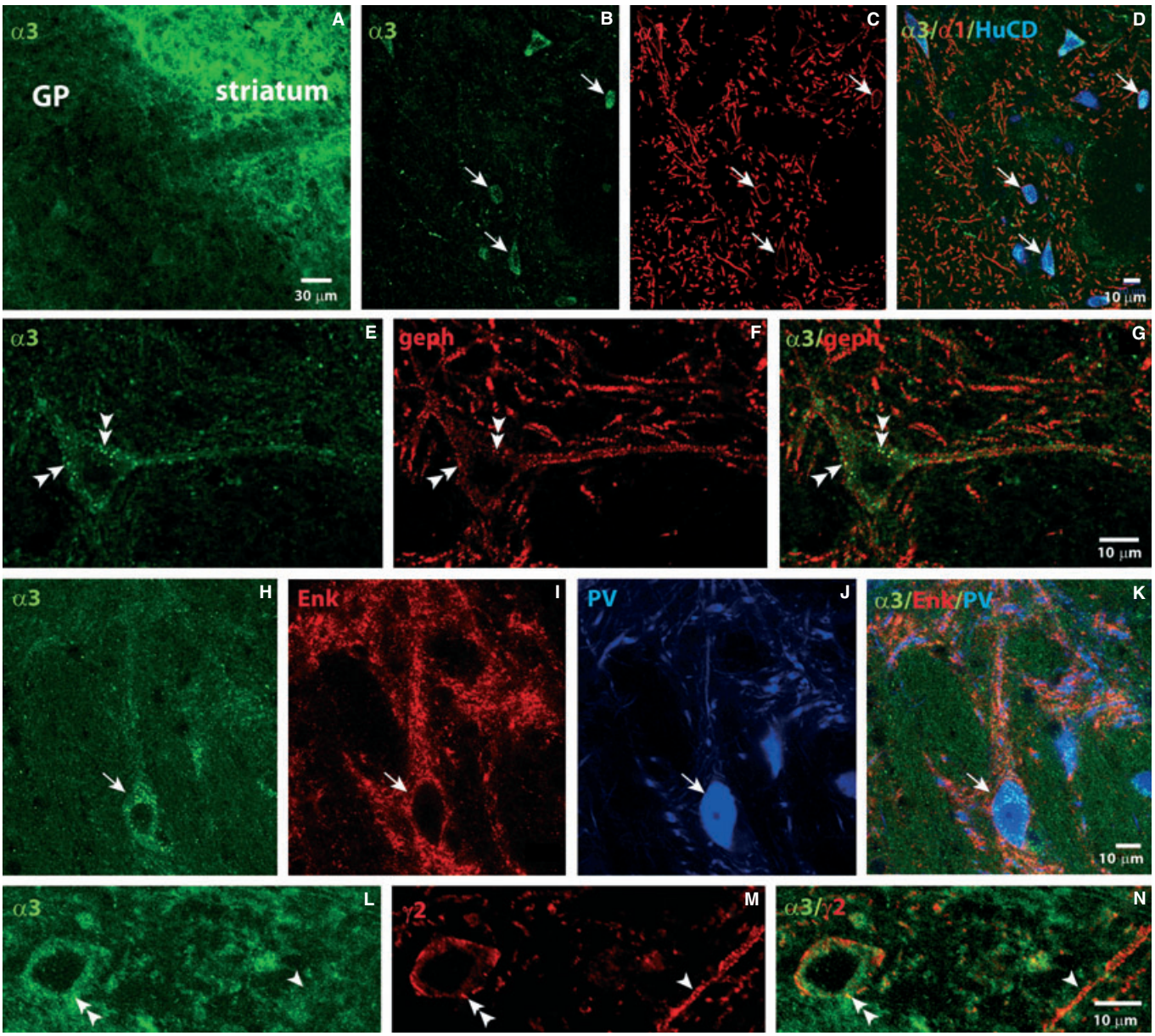

FIG. 5. Preferential localization of the GABA$_A$ α3 subunit at synapses targeting the soma of GP neurons. (A) Low power confocal image showing weak immunoreactivity for the GABA$_A$ α3 subunit in the GP and strong labeling in the striatum. (B–D) Low power images illustrating the co-localization of the two GABA$_A$ subunits, α1 (C, red) and α3 (B, green) in GP neurons (arrows), identified by the neuronal marker HuC/D (D, blue). (B) Note that GABA$_A$ α3 subunit immunoreactivity (green) is mainly present in the soma of GP neurons (arrows), as opposed to the GABA$_A$ α1 subunit immunoreactivity (red, C) which is distributed uniformly in the somatic and dendritic compartments. (E) High power image of a GP neuron displaying strong immunoreactivity for the GABA$_A$ α3 subunit (green) at the soma (double arrowheads) and weaker labeling towards more distal dendritic compartments. (F) Strong gephyrin immunoreactivity (red) at both somatic and dendritic compartments, indicating extensive inhibitory input to GP neurons. (G) Co-localization (double arrowheads) of the GABA$_A$ α3 subunit immunoreactivity (green) and gephyrin immunoreactivity (red) on the surface and intracellularly. (H–K) A GABA$_A$ α3 subunit immunoreactive (green, H) and parvalbumin-positive (blue, J) GP neuron (arrow) closely apposed by enkephalin-positive boutons (red, I) on both somatic and dendritic compartments. (L) Strong GABA$_A$ α3 subunit immunoreactivity (green) concentrated in the soma of a GP neuron (double arrowhead). Note the considerably weaker labeling observed on a nearby dendrite (arrowhead). (M) GABA$_A$ γ2 subunit immunoreactivity (red) showing strong labeling at both somatic and dendritic compartments of the same structures as in L. (N) Merged image illustrating the co-localization of the GABA$_A$ α3 subunit immunoreactivity (green) and GABA$_A$ γ2 subunit immunoreactivity (red) in the soma (double arrowhead), and the lack of co-localization on a nearby dendrite (arrowhead). Scale bar in D also applies to B and C; in G also applies to E and F; in K also applies to H–J; in N also applies to L and M.

synapses are kinetically slower and significantly different from GP-GP IPSCs (Sims *et al.*, 2008).

In order to differentiate between α-subunits pharmacologically, we initially used the hypnotic drug zolpidem at 100 and 400 nM. When tested on recombinant receptors, zolpidem displays a high affinity at α1-containing GABA$_A$ receptors (α1β2γ2, α1β3γ2: K_i = 20 nM), medium affinity at α2- and α3-containing GABA$_A$ receptors (e.g. α2β1γ2, α3β1γ2: K_i = 400 nM) and is ineffective at α5 subunit-containing receptors (α5β3γ2, α5β2γ2: K_i 5000 nM; Pritchett & Seeburg, 1990; Langer *et al.*, 1992). Furthermore, with regard to potency, an approximate 5- to 8-fold higher zolpidem concentration was required to generate a similar enhancement of GABA-induced

chloride flux in $\alpha2\beta3\gamma2$ or $\alpha3\beta3\gamma2$ receptors (see Ramerstorfer *et al.*, 2010 and references therein). We therefore maintain the concentrations of 100 and 400 nM zolpidem are good choices in order to differentiate between $\alpha1$ and $\alpha2/\alpha3$ subunit-containing receptors. This is further demonstrated by the work of Crestani *et al.*, (2000) who showed unequivocally, using mutated $\alpha1$ subunits, that zolpidem acted as a sedative exclusively through $\alpha1$-subunit containing $GABA_A$ receptors.

The $GABA_A$ $\gamma2$ subunit also appears critical for the activity of zolpidem (Cope *et al.*, 2004). Previously it has been reported that $GABA_A$ $\gamma2$ subunits are only present in the dendrites of GP neurons (Schwarzer *et al.*, 2001). Furthermore, enkephalin-positive medium spiny striatal neurons have been reported to exclusively innervate the dendritic shafts of GP neurons (Falls *et al.*, 1983; Okoyama *et al.*, 1987). This gave rise to the notion that striatal derived afferents preferentially innervate the dendrites of GP neurons and contain $GABA_A$ $\gamma2$ subunits. However, the data presented here indicate that $GABA_A$ $\gamma2$ subunits, as well as enkephalin-positive striatal axons and terminals, are more uniformly distributed over the whole GP neuronal architecture, being present in both somatic and dendritic compartments.

Using zolpidem at a concentration of 100 nM we have shown $GABA_A$ receptors containing the $\alpha1$ subunit are located at both Str-GP and GP-GP synapses. Increasing zolpidem to a nonselective concentration (400 nM) caused an increase in amplitude of GP-GP but not Str-GP IPSCs, suggesting a larger proportion of non-$\alpha1$ subunits at GP-GP synapses, a finding supported by the observations using the $GABA_A$ $\alpha3$-selective drug TP003. Thus, both $GABA_A$ $\alpha1$ and $\alpha3$ subunit-containing receptors were preferentially found in the soma and regions of proximal dendrites where they would be selectively targeted by axon collaterals of other GP neurons (see Fig. 7). This also raises the possibility of localization of $\alpha1$ alone or in combination with $\alpha3$ (see Fig. 5D; also Benke *et al.*, 2004).

Subcellular distribution of α-subunits

Using double immunolabeling we have demonstrated the co-localization of $GABA_A$ $\alpha1$ $\alpha2$ and $\alpha3$ subunits with the $GABA_A$ $\gamma2$ subunit and gephyrin, which we used as a potential marker for synaptic sites, thus indicating the synaptic localization of these α subunits. However, a significant proportion of the receptor subunits did not co-localize with gephyrin or the $\gamma2$ subunit, possibly indicating that some subunits may be located extrasynaptically. Another possible explanation is that some $GABA_A$ receptor subunits may not require gephyrin for postsynaptic clustering. However, the precise nature of these $GABA_A$ receptors remains unclear. It is currently accepted that the γ subunit is required for postsynaptic clustering, while the δ subunit confers extrasynaptic location when coupled with the $\alpha4$ or $\alpha6$ subunit (Nusser *et al.*, 1998). The activation of extrasynaptic receptors give rise to tonic background inhibitory conductance which can alter the input resistance of the neuron and influence synaptic efficacy and integration (Farrant & Nusser, 2005). However, there have been no reports indicating the presence of the δ subunit or indeed the presence of tonic inhibitory conductance in the GP. If a tonic conductance is present in GP, the results presented here would indicate that $\alpha1$, $\gamma2$ zolpidem-sensitive receptors may be involved (Semyanov *et al.*, 2003).

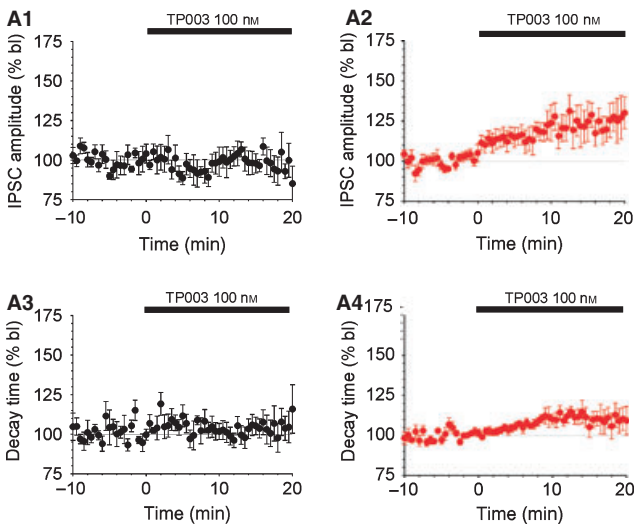

FIG. 6. The $GABA_A$ $\alpha3$ subunit was preferentially located at GP-GP synapses. 100 nM TP003 was added after 10 min of baseline recording. At Str-GP synapses (n = 7, black) TP003 had no effect on either IPSC amplitude (A/1) or decay time (A/3), while at GP-GP synapses (n = 7, red), TP003 significantly increased the IPSC amplitude (A/2).

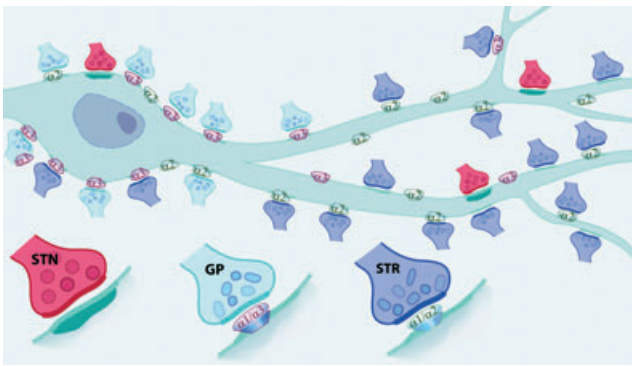

FIG. 7. Summary indicating cellular distribution of Str-GP and GP-GP synapses. A GP neuron receives its major GABAergic input from striatum (STR terminals-purple) and from neighbouring GP neurons (GP terminals; light green) and glutamatergic input from STN (STN terminals; red) and, to a lesser extent, from thalamus. Our results show an even distribution of the $GABA_A$ $\alpha1$ subunits throughout the soma and dendritic axis of GP neurons. However, there is a differential distribution of the $GABA_A$ $\alpha2$ and $\alpha3$ subunits with the $\alpha2$ preferentially located on the dendrites and $\alpha3$ preferentially located at the soma where they are targeted by local GP collaterals.

Functional implications

The activation of $GABA_A$ receptors provides inhibition on the millisecond time-scale and has therefore been implicated in regulating the temporal dynamics of neural networks (Cobb *et al.*, 1995; Traub *et al.*, 1996; Mann & Paulsen, 2007; Yamawaki *et al.*, 2008), in both physiological and pathological states. With regard to the basal ganglia and the Parkinsonian dopamine-depleted state, exaggerated oscillatory activity in the GP, amongst other nuclei, is invariably found at a frequency in the β range (~20 Hz), which is implicated in the loss of ability to perform discrete movements in both Parkinson's disease patients (Brown & Marsden, 1998; Levy *et al.*, 2000; Kuhn *et al.*, 2006) and animal models of Parkinson's disease (Mallet *et al.*, 2008). Indeed, $GABA_A$ receptor-mediated IPSPs in the STN and GP appear to not only provide tonic inhibition of downstream nuclei but also have a role in determining the timing of subsequent action potential firing by producing rebound spikes and phase realignment of the intrinsic subthreshold membrane oscillations (Bevan *et al.*, 2002; Stanford, 2003; Rav-Acha *et al.*, 2005).

It is widely accepted that perisomatic inhibition primarily controls timing of activity and ultimately the regulation of overall neuronal output (Cobb *et al.*, 1995; Miles *et al.*, 1996; Freund & Katona, 2007). Moreover, perisomatic inhibition usually involves larger

synaptic terminals, more synaptic vesicles and mitochondria, and larger active zones inducing IPSPs with faster kinetics and greater amplitude than those induced by dendrite-targeting interneurons (Miles *et al.*, 1996). This is certainly the case in the GP where perineuronal nets of GP-GP terminals activate receptors containing α1 and α3 subunits on soma and proximal dendrites, which would be expected to determine direct on/off signalling of activity. This finding also correlates with the perisomatic innervation by terminals of other PV-positive GP neurons which constitute ∼70% of the whole GP neuronal population (Kita, 1994). It remains to be determined how neuronal heterogeneity within the GP increases the complexity of the proposed schema. In contrast, dendritic inhibition may control the shunting and therefore efficacy of excitatory synaptic inputs or synaptic plasticity, perhaps through the modulation of dendritic calcium spikes (Miles *et al.*, 1996). In the hippocampus, parvalbumin-negative synapses showed five times more immunoreactivity for the $GABA_A$ α2 subunit than synapses made by parvalbumin-positive basket cells (Nyiri *et al.*, 2001; Klausberger *et al.*, 2002). This rule appears to hold in the GP, where α2 subunit-containing receptors are preferentially located at synapses targeting distal dendrites in regions where parvalbumin-positive input would be restricted.

In conclusion, our data suggest that the synapses formed by inhibitory terminals arising from the striatum and local axon collaterals from GP neurons, and which target distinct neuronal compartments are associated with different complements of $GABA_A$ receptor subunits. These data add to the growing literature that each input will mediate different physiological functions.

Supporting Information

Additional supporting information may be found in the online version of this article:

Fig. S1. GABAA α1 subunit immunoreactivity in globus pallidus neurons Triple immunofluorescent labeling for the α1 subunit (green, A), gephyrin (red, B) and VGAT (blue, C).

Table S1. Control experiments.

Please note: As a service to our authors and readers, this journal provides supporting information supplied by the authors. Suchmaterials are peer-reviewed and may be re-organized for online delivery, but are not copy-edited or typeset by Wiley-Blackwell. Technical support issues arising from supporting information (other than missing files) should be addressed to the authors.

Acknowledgements

This work was supported by The Medical Research Council UK, Grant G0300179. Many thanks to Professor Jean-Marc Fritschy for the gift of antibodies, Ben Micklem for his help with the imaging and stereology, Liz Norman, Katie Withworth and Caroline Francis for technical assistance and to Professor P. Somogyi for helpful discussions.

Abbreviations

aCSF, artificial cerebrospinal fluid; BG, basal ganglia; GP, globus pallidus; GP-GP, pallidopallidal; HuC/D, human neuronal protein; IPSC, inhibitory postsynaptic current; STN, subthalamic nucleus; Str, striatum; Str-GP, striatopallidal; VGAT, vesicular GABA transporter.

References

Amin, J. & Weiss, D.S. (1993) GABAA receptor needs two homologous domains of the beta-subunit for activation by GABA but not by pentobarbital. *Nature*, **366**, 565–569.

Barnard, E.A. (1995) The molecular biology of GABAA receptors and their structural determinants. *Adv. Biochem. Psychopharmacol.*, **48**, 1–16.

Benke, D., Fakitsas, P., Roggenmoser, C., Michel, C., Rudolph, U. & Mohler, H. (2004) Analysis of the presence and abundance of GABAA receptors containing two different types of alpha subunits in murine brain using point-mutated alpha subunits. *J. Biol. Chem.*, **279**, 43654–43660.

Bevan, M.D., Booth, P.A., Eaton, S.A. & Bolam, J.P. (1998) Selective innervation of neostriatal interneurons by a subclass of neuron in the globus pallidus of the rat. *J. Neurosci.*, **18**, 9438–9452.

Bevan, M.D., Magill, P.J., Hallworth, N.E., Bolam, J.P. & Wilson, C.J. (2002) Regulation of the timing and pattern of action potential generation in rat subthalamic neurons in vitro by GABA-A IPSPs. *J. Neurophysiol.*, **87**, 1348–1362.

Bolam, J.P., Hanley, J.J., Booth, P.A. & Bevan, M.D. (2000) Synaptic organisation of the basal ganglia. *J. Anat.*, **196**(Pt 4), 527–542.

Brown, P. & Marsden, C.D. (1998) What do the basal ganglia do? *Lancet*, **351**, 1801–1804.

Cobb, S.R., Buhl, E.H., Halasy, K., Paulsen, O. & Somogyi, P. (1995) Synchronization of neuronal activity in hippocampus by individual GAB-Aergic interneurons. *Nature*, **378**, 75–78.

Cooper, A.J. & Stanford, I.M. (2000) Electrophysiological and morphological characteristics of three subtypes of rat globus pallidus neurone in vitro. *J. Physiol.*, **527**, 291–304.

Cope, D.W., Wulff, P., Oberto, A., Aller, M.I., Capogna, M., Ferraguti, F., Halbsguth, C., Hoeger, H., Jolin, H.E., Jones, A., McKenzie, A.N., Ogris, W., Poeltl, A., Sinkkonen, S.T., Vekovischeva, O.Y., Korpi, E.R., Sieghart, W., Sigel, E., Somogyi, P. & Wisden, W. (2004) Abolition of zolpidem sensitivity in mice with a point mutation in the GABAA receptor gamma2 subunit. *Neuropharmacology*, **47**, 17–34.

Crestani, F., Martin, J.R., Möhler, H. & Rudolph, U. (2000) Mechanism of action of the hypnotic zolpidem in vivo. *Br. J. Pharmacol.*, **131**, 1251–1254.

Dias, R., Sheppard, W.F., Fradley, R.L., Garrett, E.M., Stanley, J.L., Tye, S.J., Goodacre, S., Lincoln, R.J., Cook, S.M., Conley, R., Hallett, D., Humphries, A.C., Thompson, S.A., Wafford, K.A., Street, L.J., Castro, J.L., Whiting, P.J., Rosahl, T.W., Atack, J.R., McKernan, R.M., Dawson, G.R. & Reynolds, D.S. (2005) Evidence for a significant role of alpha 3-containing GABAA receptors in mediating the anxiolytic effects of benzodiazepines. *J. Neurosci.*, **25**, 10682–10688.

Engler, B., Freiman, I., Urbanski, M. & Szabo, B. (2006) Effects of exogenous and endogenous cannabinoids on GABAergic neurotransmission between the caudate-putamen and the globus pallidus in the mouse. *J. Pharmacol. Exp. Ther.*, **316**, 608–617.

Ernst, M., Brauchart, D., Boresch, S. & Sieghart, W. (2003) Comparative modeling of GABA(A) receptors: limits, insights, future developments. *Neuroscience*, **119**, 933–943.

Essrich, C., Lorez, M., Benson, J.A., Fritschy, J.M. & Luscher, B. (1998) Postsynaptic clustering of major GABAA receptor subtypes requires the gamma 2 subunit and gephyrin. *Nat. Neurosci.*, **1**, 563–571.

Falls, W.M., Park, M.R. & Kitai, S.T. (1983) An intracellular HRP study of the rat globus pallidus. II. Fine structural characteristics and synaptic connections of medially located large GP neurons. *J. Comp. Neurol.*, **221**, 229–245.

Farrant, M. & Nusser, Z. (2005) Variations on an inhibitory theme: phasic and tonic activation of GABA(A) receptors. *Nat. Rev. Neurosci.*, **6**, 215–229.

Farrar, S.J., Whiting, P.J., Bonnert, T.P. & McKernan, R.M. (1999) Stoichiometry of a ligand-gated ion channel determined by fluorescence energy transfer. *J. Biol. Chem.*, **274**, 10100–10104.

Fornaro, M. & Geuna, S. (2005) Confocal imaging of HuC/D RNA-binding proteins in adult rat primary sensory neurons. *Ann. Anat.*, **183**, 471–473.

Freund, T.F. & Buzsaki, G. (1996) Interneurons of the hippocampus. *Hippocampus*, **6**, 347–470.

Freund, T.F. & Katona, I. (2007) Perisomatic inhibition. *Neuron*, **56**, 33–42.

Fritschy, J.M. & Mohler, H. (1995) GABAA-receptor heterogeneity in the adult rat brain: differential regional and cellular distribution of seven major subunits. *J. Comp. Neurol.*, **359**, 154–194.

Fritschy, J.M., Benke, D., Mertens, S., Oertel, W.H., Bachi, T. & Mohler, H. (1992) Five subtypes of type A gamma-aminobutyric acid receptors identified in neurons by double and triple immunofluorescence staining with subunit-specific antibodies. *Proc. Natl Acad. Sci. USA*, **89**, 6726–6730.

Fritschy, J.M., Harvey, R.J. & Schwarz, G. (2008) Gephyrin: where do we stand, where do we go? *Trends Neurosci.*, **31**, 257–264.

Gronborg, M., Pavlos, N.J., Brunk, I., Chua, J.J., Munster-Wandowski, A., Riedel, D., Ahnert-Hilger, G., Urlaub, H. & Jahn, R. (2010) Quantitative comparison of glutamatergic and GABAergic synaptic vesicles unveils selectivity for few proteins including MAL2, a novel synaptic vesicle protein. *J. Neurosci.*, **30**, 2–12.

Hoover, B.R. & Marshall, J.F. (2002) Further characterization of preproenkephalin mRNA-containing cells in the rodent globus pallidus. *Neuroscience*, **111**, 111–125.
Jacob, T.C., Bogdanov, Y.D., Magnus, C., Saliba, R.S., Kittler, J.T., Haydon, P.G. & Moss, S.J. (2005) Gephyrin regulates the cell surface dynamics of synaptic GABAA receptors. *J. Neurosci.*, **25**, 10469–10478.
Jiang, Z.G. & North, R.A. (1991) Membrane properties and synaptic responses of rat striatal neurones in vitro. *J. Physiol.* **443**, 533–553.
Kasugai, Y., Swinny, J.D., Roberts, J.D.B., Dalezios, Y., Fukazawa, Y., Sieghart, W., Shigemoto, R. & Somogyi, P. (2010) Quantitative localisation of synaptic and extrasynaptic GABAA receptor subunits on hippocampal pyramidal cells by freeze-fracture replica immunolabelling. *Eur. J. Neurosci.*, **32**, 1868–1888.
Kincaid, A.E., Penney J.B., Jr, Young, A.B. & Newman, S.W. (1991) Evidence for a projection from the globus pallidus to the entopeduncular nucleus in the rat. *Neurosci. Lett.*, **128**, 121–125.
Kita, H. (1994) Parvalbumin-immunopositive neurons in rat globus pallidus: a light and electron microscopic study. *Brain Res.*, **657**, 31–41.
Kita, H. & Kitai, S.T. (1994) The morphology of globus pallidus projection neurons in the rat: an intracellular staining study. *Brain Res.*, **636**, 308–319.
Klausberger, T., Roberts, J.D. & Somogyi, P. (2002) Cell type- and input-specific differences in the number and subtypes of synaptic GABA(A) receptors in the hippocampus. *J. Neurosci.*, **22**, 2513–2521.
Kneussel, M., Brandstätter, J.H., Gasnier, B., Feng, G., Sanes, J.R. & Betz, H. (2001) Gephyrin-independent clustering of postsynaptic GABA(A) receptor subtypes. *Mol. Cell. Neurosci.*, **6**, 973–982.
Kuhn, A.A., Kupsch, A., Schneider, G.H. & Brown, P. (2006) Reduction in subthalamic 8–35 Hz oscillatory activity correlates with clinical improvement in Parkinson's disease. *Eur. J. Neurosci.*, **23**, 1956–1960.
Langer, S.Z., Faure-Halley, C., Seeburg, P., Graham, D. & Arbilla, S. (1992) The selectivity of zolpidem and alpidem for the α1-subunit of GABAA receptor. *Eur. Neuropsyhocopharmacol.*, **2**, 232–234.
Langer, S.Z., Seeburg, P., Graham, D. & Arbilla, S. (1992) The selectivity of zolpidem and alpidem for the alpha1-subunit of the GABAA receptor. *Eur. Neuropsychopharmacol.*, **2**, 232–234.
Lavoie, A.M., Tingey, J.J., Harrison, N.L., Pritchett, D.B. & Twyman, R.E. (1997) Activation and deactivation rates of recombinant GABA(A) receptor channels are dependent on alpha-subunit isoform. *Biophys. J.*, **73**, 2518–2526.
Lévi, S., Logan, S.M., Tovar, K.R. & Craig, A.M. (2004) Gephyrin is critical for glycine receptor clustering but not for the formation of functional GABAergic synapses in hippocampal neurons. *J. Neurosci.*, **24**, 207–217.
Levitan, E.S., Blair, L.A., Dionne, V.E. & Barnard, E.A. (1988) Biophysical and pharmacological properties of cloned GABAA receptor subunits expressed in Xenopus oocytes. *Neuron*, **1**, 773–781.
Levy, R., Hutchison, W.D., Lozano, A.M. & Dostrovsky, J.O. (2000) High-frequency synchronization of neuronal activity in the subthalamic nucleus of parkinsonian patients with limb tremor. *J. Neurosci.*, **20**, 7766–7775.
Lindemeyer, K., Leemhuis, J., Löffler, S., Grass, N., Nöremberg, W. & Meyer, D.K. (2006) Metabotropic glutamate receptors modulate the NMDA- and AMPA-induced gene expression in neocortical interneurons. *Cereb. Cortex.*, **16**, 1662–1677.
Mann, E.O. & Paulsen, O. (2007) Role of GABAergic inhibition in hippocampal network oscillations. *Trends Neurosci.*, **30**, 343–349.
Mallet, N., Pogosyan, A., Sharott, A., Csicsvari, J., Bolam, J.P., Brown, P. & Magill, P.J. (2008) Disrupted dopamine transmission and the emergence of exaggerated beta oscillations in subthalamic nucleus and cerebral cortex. *J. Neurosci.*, **28**, 4795–4806.
McKernan, R.M., Rosahl, T.W., Reynolds, D.S., Sur, C., Wafford, K.A., Atack, J.R., Farrar, S., Myers, J., Cook, G., Ferris, P., Garrett, L., Bristow, L., Marshall, G., Macaulay, A., Brown, N., Howell, O., Moore, K.W., Carling, R.W., Street, L.J., Castro, J.L., Ragan, C.I., Dawson, G.R. & Whiting, P.J. (2000) Sedative but not anxiolytic properties of benzodiazepines are mediated by the GABA(A) receptor alpha1 subtype. *Nat. Neurosci.*, **3**, 87–592.
Miles, R., Toth, K., Gulyas, A.I., Hajos, N. & Freund, T.F. (1996) Differences between somatic and dendritic inhibition in the hippocampus. *Neuron*, **16**, 815–823.
Nambu, A. & Llinas, R. (1994) Electrophysiology of globus pallidus neurons in vitro. *J. Neurophysiol.*, **72**, 1127–1139.
Newell, J.G. & Dunn, S.M. (2002) Functional consequences of the loss of high affinity agonist binding to gamma-aminobutyric acid type A receptors. Implications for receptor desensitization. *J. Biol. Chem.*, **277**, 21423–21430.
Nusser, Z., Sieghart, W. & Somogyi, P. (1998) Segregation of different GABAA receptors to synaptic and extrasynaptic membranes of cerebellar granule cells. *J. Neurosci.*, **18**, 1693–1703.
Nyiri, G., Freund, T.F. & Somogyi, P. (2001) Input-dependent synaptic targeting of alpha(2)-subunit-containing GABA(A) receptors in synapses of hippocampal pyramidal cells of the rat. *Eur. J. Neurosci.*, **13**, 428–442.
Okoyama, S., Nakamura, Y., Moriizumi, T. & Kitao, Y. (1987) Electron microscopic analysis of the synaptic organization of the globus pallidus in the cat. *J. Comp. Neurol.*, **265**, 323–331.
Parent, A. & Hazrati, L.N. (1995) Functional anatomy of the basal ganglia. II. The place of subthalamic nucleus and external pallidum in basal ganglia circuitry. *Brain Res. Rev.*, **20**, 128–154.
Pirker, S., Schwarzer, C., Wieselthaler, A., Sieghart, W. & Sperk, G. (2000) GABA(A) receptors: immunocytochemical distribution of 13 subunits in the adult rat brain. *Neuroscience*, **101**, 815–850.
Pritchett, D.B. & Seeburg, P.H. (1990) Gamma-aminobutyric acidA receptor alpha 5-subunit creates novel type II benzodiazepine receptor pharmacology. *J. Neurochem.*, **54**, 1802–1804.
Ramerstorfer, J., Furtmüller, R., Vogel, E., Huck, S. & Sieghart, W. (2010) The point mutation gamma 2F77I changes the potency and efficacy of benzodiazepine site ligands in different GABAA receptor subtypes. *Eur. J. Pharmacol.*, **636**, 18–27.
Ramming, M., Kins, S., Werner, N., Hermann, A., Betz, H. & Kirsch, J. (2000) Diversity and phylogeny of gephyrin: tissue-specific splice variants, gene structure, and sequence similarities to molybdenum cofactor-synthesizing and cytoskeleton-associated proteins. *Proc. Natl Acad. Sci. USA*, **97**, 10266–10271.
Rav-Acha, M., Sagiv, N., Segev, I., Bergman, H. & Yarom, Y. (2005) Dynamic and spatial features of the inhibitory pallidal GABAergic synapses. *Neuroscience*, **135**, 791–802.
Sadek, A.R., Magill, P.J. & Bolam, J.P. (2007) A single-cell analysis of intrinsic connectivity in the rat globus pallidus. *J. Neurosci.*, **27**, 6352–6362.
Sato, F., Lavallee, P., Levesque, M. & Parent, A. (2000) Single-axon tracing study of neurons of the external segment of the globus pallidus in primate. *J. Comp. Neurol.*, **417**, 17–31.
Schneider Gasser, E.M., Straub, C.J., Panzanelli, P., Weinmann, O., Sassoe-Pognetto, M. & Fritschy, J.M. (2006) Immunofluorescence in brain sections: simultaneous detection of presynaptic and postsynaptic proteins in identified neurons. *Nat. Protoc.*, **1**, 1887–1897.
Schwarzer, C., Berresheim, U., Pirker, S., Wieselthaler, A., Fuchs, K., Sieghart, W. & Sperk, G. (2001) Distribution of the major gamma-aminobutyric acid(A) receptor subunits in the basal ganglia and associated limbic brain areas of the adult rat. *J. Comp. Neurol.*, **433**, 526–549.
Semyanov, A., Walker, M.C. & Kullmann, D.M. (2003) GABA uptake regulates cortical excitability via cell type-specific tonic inhibition. *Nat. Neurosci.*, **6**, 484–490.
Shink, E., Bevan, M.D., Bolam, J.P. & Smith, Y. (1996) The subthalamic nucleus and the external pallidum: two tightly interconnected structures that control the output of the basal ganglia in the monkey. *Neuroscience*, **73**, 335–357.
Sieghart, W. (1995) Structure and pharmacology of gamma-aminobutyric acidA receptor subtypes. *Pharmacol. Rev.*, **47**, 181–234.
Sigel, E. (2002) Mapping of the benzodiazepine recognition site on GABA(A) receptors. *Curr. Top. Med. Chem.*, **2**, 833–839.
Sims, R.E., Woodhall, G.L., Wilson, C.L. & Stanford, I.M. (2008) Functional characterization of GABAergic pallidopallidal and striatopallidal synapses in the rat globus pallidus in vitro. *Eur. J. Neurosci.*, **28**, 2401–2408.
Smith, Y. & Bolam, J.P. (1989) Neurons of the substantia nigra reticulata receive a dense GABA-containing input from the globus pallidus in the rat. *Brain Res.*, **493**, 160–167.
Smith, Y., Bolam, J.P. & Von Krosigk, M. (1990) Topographical and synaptic organization of the GABA-containing pallidosubthalamic projection in the rat. *Eur. J. Neurosci.*, **2**, 500–511.
Stanford, I.M. (2003) Independent neuronal oscillators of the rat globus pallidus. *J. Neurophysiol.*, **89**, 1713–1717.
Traub, R.D., Whittington, M.A., Colling, S.B., Buzsaki, G. & Jefferys, J.G. (1996) Analysis of gamma rhythms in the rat hippocampus in vitro and in vivo. *J. Physiol.*, **493**, 471–484.
Tretter, V., Ehya, N., Fuchs, K. & Sieghart, W. (1997) Stoichiometry and assembly of a recombinant GABAA receptor subtype. *J. Neurosci.*, **17**, 2728–2737.
Voorn, P., van de Witte, S., Tjon, G. & Jonker, A.J. (1999) Expression of enkephalin in pallido-striatal neurons. *Ann. N Y Acad. Sci.*, **877**, 671–675.
Wilson, C.J. & Phelan, K.D. (1982) Dual topographic representation of neostriatum in the globus pallidus of rats. *Brain Res.*, **243**, 354–359.
Yamawaki, N., Stanford, I.M., Hall, S.D. & Woodhall, G.L. (2008) Pharmacologically induced and stimulus evoked rhythmic neuronal oscillatory activity in the primary motor cortex in vitro. *Neuroscience*, **151**, 386–395.